Theor Chem Acc (2002) 108:85–97
DOI 10.1007/s00214-002-0337-y

Theoretical
Chemistry Accounts

Regular article

Infrared spectra of CO in absorption and evaluation of radial functions for potential energy and electric dipolar moment

J. F. Ogilvie[1], **S.-L. Cheah**[2], **Y.-P. Lee**[2], **S. P. A. Sauer**[3]

[1] Centre for Experimental and Constructive Mathematics, Department of Mathematics, Simon Fraser University, 8888 University Drive, Burnaby BC V5A 1S6, Canada
[2] Department of Chemistry, National Tsing Hua University, 101, Section 2, Kuang-Fu Road, Hsinchu 30013, Taiwan
[3] Department of Chemistry, University of Copenhagen, Universitetsparken 5, 2100 Copenhagen O, Denmark

Received: 8 November 2001 / Accepted: 5 February 2002 / Published online: 14 August 2002

Abstract. From quantum-chemical calculations of rotational g factor and new experimental measurements of strengths of lines in infrared spectra of vibration–rotational bands v'–0 in absorption, with $1 \le v' \le 4$, of $^{12}C^{16}O$, and from analysis of 16,947 frequencies and wave numbers assigned to pure rotational and vibration–rotational transitions within electronic ground state $X\ ^1\Sigma^+$, including new measurements of band 4–0 of $^{12}C^{16}O$, we evaluate radial functions for potential energy and electric dipolar moment, the latter both in polynomial form and as a rational function that has qualitatively correct behaviour under limiting conditions.

Key words: Vibration–rotational spectra – Rotational g factor – Analysis of frequencies – Analysis of intensities

1 Introduction

Although CO is only a minor constituent of the contemporary native terrestrial atmosphere, this chemical compound is an important component of fumes from incomplete combustion of fuels comprising carbon and its compounds under diverse conditions. Beyond this planet CO has been detected in the solar photosphere, innumerable stars and interstellar clouds [1]. From its first spectral detection through absorption in the mid-infrared region in 1889, when CO became the first diatomic compound in the gaseous phase for which such observations were made [2], spectral measurements have played a dominant role in monitoring its presence under diverse conditions. Whereas for remote astronomical objects detection of CO in several isotopic variants in the microwave spectral region is preferable, observation either of light from or through exhaust fumes from stationary or mobile combustors or of radiant emission from lasers or comparable systems of gaseous plasmas is common in mid- and near-infrared regions. For all such monitoring, an accurate knowledge of both frequencies and intensities of spectral transitions is essential. During the twentieth century the fundamental band in the mid-infrared region was first measured as a doublet with unresolved lines in each rotational branch; as spectral instruments improved, lines became increasingly well resolved and precision of wave numbers characterising these lines increased correspondingly. Since 1924 there have been numerous attempts to measure, first, an integrated intensity of a band containing unresolved or poorly resolved lines and, subsequently, intensities of individual lines; compilations [3, 4, 5] of results of such measurements indicate that reports of values for CO as either its most common species $^{12}C^{16}O$ or an isotopic variant are more numerous than those for any other diatomic molecular compound. For the fundamental band near $2.15\times10^5\ m^{-1}$ such integrated intensities described as band strength range over nearly a factor two, whereas for the first-overtone band near $4.26\times10^5\ m^{-1}$ the corresponding range is over a factor three. Despite these many measurements of band strengths, few of them are based on individually resolved lines; problematic measurement of bands resulting from gaseous samples at elevated densities is reflected in diverse magnitudes of band strengths.

With a contemporary instrument for the infrared region that is based on either an interferometer or tunable diode lasers, one can achieve spectral resolution of order $0.1\ m^{-1}$; under such conditions essentially complete resolution of an individual line not too near a band head might be attainable, depending on details of species, frequency and condition of sample. A strength of that line is then directly measurable with relative precision of order 1%. Even with maximum resolution about $0.4\ m^{-1}$ obtained with a commercial instrument, in previous investigations of gaseous HCl [6] and O_2 [7] in this laboratory we measured line strengths, through direct integration of areas of individual spectral lines displayed as absorbance, that agreed satisfactorily with

Correspondence to: J. F. Ogilvie
e-mail: ogilvie@cecm.sfu.ca

preceding or concurrent measurements according to complicated protocols. Such an exercise in metrology serves a useful purpose in producing standards that are applicable for both monitoring purposes and quantitative analysis. For absorption bands attributed to transitions involving only vibrational and rotational quantum numbers within a single electronic state, data in terms of measured properties of lines can be reduced to parameters in one or other radial function, according to which some molecular property varies with internuclear distance. For measurements of frequencies of individual lines, the dominant corresponding molecular property is potential energy, but other functions exert minor influences that become significant with spectral resolution or line width $\delta\nu$ at frequency ν such that $\nu/\delta\nu \sim 10^6$, and with multiple isotopic species. For measurements of integrated intensities of relatively intense lines in absorption for compounds comprising electrically dipolar molecules, the ratio of line strength, S_l, to its uncertainty, δS_l, is typically $S_l/\delta S_l \sim 10^2$ at best; the pertinent molecular property is electric dipolar moment, but few, if any, imprecise measurements of spectral intensities indicate a need for auxiliary radial functions.

In this project we undertook measurement of strengths of lines in four bands of gaseous CO in absorption, specifically from the vibrational ground state $v=0$ to the first four vibrationally excited states, $1 \leq v' \leq 4$, according to limits imposed by our apparatus; these measurements provide a consistent basis for evaluation of a radial function for electric dipolar moment. That our work is timely is demonstrated by facts that, during a period since our initial measurements in this project on CO, reports of two independent measurements of intensity of the second-overtone band have appeared [8, 9] and that other authors [10] derived a function for electric dipolar moment based on old measurements of intensities. Accurate frequencies or wave numbers for a few isotopic species involving spectral transitions up to $v'=41$ are available in the literature; analysis of these data not only enables evaluation of a function for potential energy that is required for analysis of intensities but also might furnish information about other properties. Recent measurements [11, 12, 13, 14] of highly precise frequencies of pure rotational transitions enable delineation of isotopic effects to be improved since a previous report of such calculations [15]. The rotational g factor [16], g_r, and electric dipolar moment, p, are molecular properties that one can calculate at various internuclear distances; this information not only is helpful during evaluation of potential energy from frequency data but also enables estimation of other properties that are not yet routinely calculable with quantum-chemical methods. Results of such calculations of electric dipolar moment can be tested with results derived independently from measurements of spectral intensities.

We describe here our experiments and calculations that yield new and definitive evaluations of radial functions for CO. A pertinent aspect of our procedure is direct application of symbolic computation, which greatly facilitates analysis of spectra of diatomic molecules [2]. We employ SI units in conformity to recommendation of IUPAC.

2 Experiments

We recorded all spectra with an evacuated interferometric spectrometer (Bomem DA8, at National Tsing Hua University) in conjunction with one or other vessel containing gaseous CO (Air Products, nominal purity 99.9%, used without purification). One vessel was a simple tube (length 0.100 m) enclosed with KBr crystals as windows to transmit infrared radiation. Another vessel (Infrared Analysis, model 100), employing multiple internal reflections, had a path of maximum length 107 m through absorbing sample; the number of passes of the beam, with distance 1.375 m between mirrors in each pass, through a sample at a particular pressure and temperature is adjustable to produce optimal absorption. For measurements of fundamental band and first and second overtones, we employed a beam splitter made of CaF_2 and an InSb detector cooled to 77 K, but for the third overtone we used a quartz beam splitter and a Ge detector; for the fundamental band the source was a SiC rod, whereas for the other bands the source was a tungsten filament. To limit radiation reaching the detector to a region of interest, we employed optical filters (supplier, part number and pass band/10^5 m^{-1}) as follows: Spectrogon LP4000, 1.2–2.4; OCLI W02296–7, 3.9–5.0; Omega 1775WB450, 5.1–6.5; Omega 1200WB200, 7.6–8.9. Spectral resolution was 0.4–1.0 m^{-1} for the fundamental and first-overtone bands and 0.8–2.0 m^{-1} for the second- and third-overtone bands, according to need. We calibrated the wave number scale with standard gases [17].

Each interferogram, coadded from numerous scans, was accumulated over several hours, during which we monitored the temperature of the container of gaseous sample with one – for the short vessel – or two – for the long vessel – thermocouples of type K to indicate maximum and minimum temperatures. The pressure of each sample was measured with capacitance manometers (MKS model 122AA) with a range apt for a particular sample. Fourier transform of an interferogram, conversion to absorbance with a reference spectrum, and fitting stature, width and area of, generally, each individual spectral line were effected with software provided with the spectrometer (proprietary, and Grams from Galactic Industries). For the most intense lines in a band, conditions of partial pressure of absorbing gas and of resolution were set so that a ratio of signal to noise, measured quantitatively during fitting of line profiles, was about 200, except for band 4–0, for which a smaller ratio had to be tolerated; under optimal conditions an area of each spectral line, or a corresponding line strength, had a relative precision about 1% for the most intense lines in a band, degrading to 20% for the least acceptable weak lines. Statistical weighting of all measurements was carried through the analysis to obtain the final coefficients of radial functions.

Conditions of measurement peculiar to each band were as follows. The strengths of intense lines in the fundamental band are sufficiently large that, with an absorbing path of length 0.1 m, the partial pressure of CO need be only about 5 N m^{-2}, which is inconveniently small to be measured accurately; for this reason we diluted a sample with Ar or He at 1:100 or 1:1000, allowing time for thorough mixing and with accurately

measured pressures. This presence of Ar or He in the absorption cell at total pressures up to 13,000 N m^{-2} causes broadening of spectral lines, up to 7 m^{-1}; we are thereby able to decrease spectral resolution and to increase the range of absorbance without problems of saturation and consequent distortion of lines. For the first overtone we made measurements on both pure CO and CO diluted with He in a cell with an absorbing path of length 0.1 m, with pressures in a range/N m^{-2} [650, 6500]. For the second overtone, we employed only pure CO in a vessel with length of absorbing path adjustable up to 107 m; for intense lines of $^{12}C^{16}O$ an absorbing path of length 8.25 m with pressure 2,620 N m^{-2} sufficed, whereas for lines of isotopic variants the length of absorbing path and pressure were increased accordingly. Although considerable effort was invested in measuring intensities of lines of isotopic variants, inaccuracy of their independently measured concentrations and the possibility of variation of isotopic ratios during purification preclude their use to extend the analysis at present. For the third overtone, the length of absorbing path was almost the maximum practicable; we employed pressures of pure CO in a range/N m^{-2} [27000, 108000] producing broadening of lines having widths up to 18 m^{-1} at the greatest pressures.

3 Quantum-chemical calculations

According to separate treatment of electronic and nuclear motions that corresponds to the Born–Oppenheimer approximation, the electric dipolar moment, $\vec{p}$, of a molecule in an electronic state described with an electronic wave function $|\Psi_0\rangle$ comprises nuclear, p^{n}, and electronic, p^{el}, contributions; the nuclear contribution depends on only position vectors and charges of atomic nuclei, whereas the electronic contribution involves an expectation value of the corresponding electronic wave function. For CO the vector for dipolar moment is then

$$\vec{p} = e(Z_{\mathrm{C}}\vec{r}_{\mathrm{C}} + Z_{\mathrm{O}}\vec{r}_{\mathrm{O}}) - e\left\langle \Psi_0 \left| \sum_{i=1}^{14} \vec{r}_i \right| \Psi_0 \right\rangle \ , \qquad (1)$$

in which Z_{C} and Z_{O} are atomic numbers, $\vec{r}_{\mathrm{C}}$ and $\vec{r}_{\mathrm{O}}$ are position vectors of atomic nuclei of carbon and oxygen respectively, and $\vec{r}_i$ is a position vector of an electron. The rotational g factor, g_{r} [16], also comprises nuclear, $g_{\mathrm{r}}^{\mathrm{n}}$, and electronic, $g_{\mathrm{r}}^{\mathrm{el}}$ contributions. For a diatomic molecule such as CO the nuclear contribution depends on only masses, M_{C} and M_{O}, and atomic numbers of atoms and the protonic rest mass, m_{p},

$$g_{\mathrm{r}}^{\mathrm{n}} = m_{\mathrm{p}} \frac{Z_{\mathrm{C}}M_{\mathrm{O}}^2 + Z_{\mathrm{O}}M_{\mathrm{C}}^2}{M_{\mathrm{C}}M_{\mathrm{O}}(M_{\mathrm{C}} + M_{\mathrm{O}})} \ , \qquad (2)$$

and is thus independent of internuclear distance, R. As given by perturbation theory to second order, the electronic contribution, $g_{\mathrm{r}}^{\mathrm{el}}$, involves summation over all excited electronic states $|\Psi_n\rangle$ each with energy E_n. For a diatomic molecule, this quantity is expressed as

$$g_{\mathrm{r}}^{\mathrm{el}} = \frac{2m_{\mathrm{p}}}{m_{\mathrm{e}}\mu R^2} \sum_{n\neq 0} \frac{\left\langle \Psi_0 \left| \sum_{i=1}^{14} l_{i,\perp}(\vec{R}_{\mathrm{CM}}) \right| \Psi_n \right\rangle \left\langle \Psi_n \left| \sum_{i=1}^{14} l_{i,\perp}(\vec{R}_{\mathrm{CM}}) \right| \Psi_0 \right\rangle}{E_0 - E_n} \ , \qquad (3)$$

in which reduced mass for CO is defined as $\mu = M_{\mathrm{C}}M_{\mathrm{O}}/(M_{\mathrm{C}} + M_{\mathrm{O}})$, m_{e} is electronic rest mass and $l_{i,\perp}(\vec{R}_{\mathrm{CM}})$ is an operator for orbital angular momentum of electron i defined with respect to the centre of mass of a molecule. An expression containing a sum over states such as in Eq. (3) can be conveniently – i.e. without explicit calculation of excited electronic states $|\Psi_n\rangle$ – evaluated with polarization-propagator or linear-response functions [18, 19]. We employed a multiconfigurational self-consistent-field (MCSCF) ansatz for an electronic wave function $|\Psi_0\rangle$ of electronic ground state $X\ ^1\Sigma^+$ to calculate electronic contributions to both electric dipolar moment, p^{el}, as the second term on the right side of Eq. (1), and rotational g factor, $g_{\mathrm{r}}^{\mathrm{el}}$, in Eq. (3).

We expanded molecular orbitals in a set of one-electron basis functions that comprise 10 *s*-, 8 *p*-, 6 *d*-, 2 *f*- and 1 *g*-type spherical gaussian functions centred on both atoms, in total 174 gaussian basis functions. Basis sets of *s* and *p* types were derived from the 11*s*7*p* basis sets of van Duijneveldt [20] on contracting functions of *s* type with the five largest exponents to a single contracted gaussian function using coefficients of the 1*s* atomic orbital obtained in the corresponding Hartree–Fock calculations of van Duijneveldt [20]. Functions of *s* type with the three smallest exponents were replaced by six *s* functions with exponents $\zeta_s = 1.092350$, 0.437465, 0.175196, 0.070163, 0.0280988, 0.0112530 for carbon and with exponents $\zeta_s = 2.130353$, 0.842602, 0.333268, 0.131815, 0.0521357, 0.0206208 for oxygen; two diffuse functions of *p* type were added with exponents $\zeta_p = 0.0301449$, 0.0117542 for carbon and with exponents $\zeta_p = 0.0536415$, 0.0190886 for oxygen. Polarization functions 3d2*f*1*g* were taken from cc-pVQZ basis sets of Dunning [21] augmented with two additional functions of d type with exponents $\zeta_d = 5.262$, 0.028 for carbon and $\zeta_d = 10.962$, 0.052 for oxygen. The type of MCSCF wave function was complete active space [22]. In initial calculations at a preliminary equilibrium internuclear distance of 1.1283228×10^{-10} m, we tested four active spaces, presented in Table 1, whereas in calculating radial functions we used only the 3–7 σ 1–2 π active space. Program system Dalton 1.1 [23] served for all calculations, the results of which appear in Tables 1 and 2.

4 Analysis of frequency data

The wave numbers of lines in branches P and R of band 4–0 of $^{12}C^{16}O$ measured at resolution 0.8 m^{-1} appear in Table 3; the spectrum is depicted in Fig. 1. Precision of

Table 1 Dependence of rotational g factor g_r and electric dipolar moment $\vec{p}$ on active space of CO in electronic ground state $X\ ^1\Sigma^+$ at $R / 10^{-10}$ m = 1.1283228

active space	No. of determinants	g_r	$\vec{p}$ / 10^{-30} C m
3-5 σ 1 π [a]	1	-0.28000	-0.88548
3-6 σ 1-2 π [b]	792	-0.25770	1.15585
3-7 σ 1-2 π	4076	-0.25412	0.68480
3-9 σ 1-4 π 1 δ	9576560	-0.25636	0.02535

[a] calculation with a self-consistent field (SCF)
[b] a valence complete active space including valence orbitals (2s and 2p) on both atoms

Table 2 Molecular properties of $^{12}C^{16}O$ in electronic ground state $X\ ^1\Sigma^+$ calculated at varied internuclear distance

$R / 10^{-10}$ m	energy / hartree [a]	g_r	$\vec{p}$ / 10^{-30} C m [b]
0.84	-112.5528457432	- 0.27327	3.55701
0.88	-112.6851945199	- 0.25864	3.20210
0.92	-112.7815093815	- 0.24979	2.82677
0.96	-112.8497221941	- 0.24526	2.43473
1	-112.8960542389	- 0.24399	2.02963
1.04	-112.9253959406	- 0.24521	1.61513
1.08	-112.9415999319	- 0.24835	1.19494
1.1283228	-112.9479409951	- 0.25412	0.68480
1.16	-112.9461203040	- 0.25885	0.35168
1.2	-112.9387399939	- 0.26570	- 0.06452
1.25	-112.9236246338	- 0.27541	- 0.57331
1.31	-112.8997404070	- 0.28849	- 1.15950
1.38	-112.8675125885	- 0.30539	- 1.79953
1.46	-112.8281722501	- 0.32646	- 2.46008
1.54	-112.7891329943	- 0.34889	- 3.03474
1.62	-112.7519243300	- 0.37214	- 3.51708
1.7	-112.7174381435	- 0.39569	- 3.90352
1.8	-112.6788107271	- 0.42502	- 4.24562
1.9	-112.6454392249	- 0.45450	- 4.41273
2	-112.6173659249	- 0.48005	- 4.24782
2.1	-112.5947682326	- 0.51473	- 3.86486

[a] for conversion to SI units, 1 hartree = 21947463.13710 m^{-1}
[b] The polarity of CO at internuclear distance 10^{-10} m is taken as $^-CO^+$.

wave numbers in Table 3 is 0.088 m^{-1}, except for a few weak lines at the end of each branch for which uncertainty increases to 0.4 m^{-1}. These wave numbers are combined with those employed in a preceding analysis of frequency data [15], to which are added data of $^{14}C^{16}O$ [24, 25] previously [15] omitted, frequencies of lines of pure rotational transitions of isotopic variants measured precisely in the sub-millimetre region [11, 12, 13, 14] and also for $^{12}C^{17}O$ and $^{13}C^{17}O$ (G. Winnewisser, personal communication), with other precise data [26, 27]. We fitted in total 16,947 frequencies and wave numbers of pure rotational and vibration–rotational transitions of CO in isotopic variants with $^{12,13,14}C$ and $^{16,17,18}O$ in various combinations to parameters in several radial functions defined according to an effective hamiltonian of form [28, 29]

$$H_{\text{eff}} = (-\hbar^2/2\mu)\mathrm{d}/\mathrm{d}R[1 + \beta(R)]\mathrm{d}/\mathrm{d}R + V(R) + V'(R) + (\hbar^2/2\mu R^2)[1 + \alpha(R)]J(J+1) \ , \quad (4)$$

in which $\hbar$ is Planck's constant, h, divided by 2π. In these functions we employ a coordinate z for reduced displacement from equilibrium separation,

$$z \equiv 2(R - R_e)/(R + R_e) \ , \quad (5)$$

with R as instantaneous internuclear distance and R_e as equilibrium internuclear separation. Besides a function of potential energy of form [2]

Table 3 Wave number $\tilde{\nu}$ /m^{-1} of lines measured in band 4 – 0 of $^{12}C^{16}O$ $X\ ^1\Sigma^+$

J	P(J")	R(J")
0	—	841817.756
1	841062.798	842174.135
2	840664.053	842516.521
3	840251.535	842844.870
4	839825.154	843159.220
5	839384.735	843459.479
6	838930.419	843745.627
7	838462.258	844017.713
8	837980.088	844275.670
9	837484.169	844519.491
10	836974.230	844749.209
11	836450.576	844964.690
12	835912.974	845166.043
13	835361.645	845353.208
14	834796.437	845526.094
15	834217.370	845684.794
16	833624.651	845829.311
17	833018.227	845959.553
18	832398.011	846075.496
19	831763.729	846177.108
20	831115.564	846264.571
21		846337.536
22		846396.349
23		846440.912
24		846471.133
25		846486.321

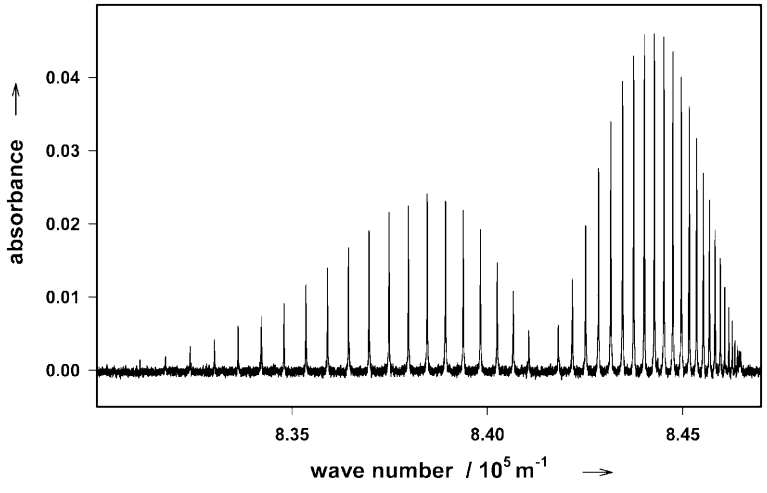

Fig. 1. Absorption spectrum of $^{12}C^{16}O$; length of absorbing path = 107.25 m and pressure of gas = 1.067×10^5 N m^{-2}

$$V(R) \rightarrow V(z) = c_0 z^2 \left(1 + \sum_{j=1} c_j z^i\right) , \qquad (6)$$

which is formally independent of nuclear mass, three associated radial functions that depend formally on mass of an atomic nucleus of each type take into account nonadiabatic vibrational effects,

$$\beta(R) \rightarrow m_e \left(\sum_{j=0} s_j^C z^j \Big/ M_C + \sum_{j=0} s_j^O z^j \Big/ M_O\right) , \qquad (7)$$

nonadiabatic rotational effects,

$$\alpha(R) \rightarrow m_e \left(\sum_{j=0} t_j^C z^j \Big/ M_C + \sum_{j=0} t_j^O z^j \Big/ M_O\right) , \qquad (8)$$

and adiabatic effects,

$$V'(R) \rightarrow m_e \left(\sum_{j=1} u_j^C z^j \Big/ M_C + \sum_{j=1} u_j^O z^j \Big/ M_O\right) . \qquad (9)$$

Table 4 Fitted spectral and molecular parameters and radial coefficients for CO $X\ ^1\Sigma^+$

$U_{1,0}$ / m^{-1} u^{½} = 568137.9691 ± 0.0183	k_e / N m^{-1} = 1901.769072 ± 0.000193
$U_{0,1}$ / m^{-1} u = 1324.346399 ± 0.000030	R_e / 10^{-10} m = 1.12822950 ± 0.00000089
c_0 / m^{-1} = 60932085.46 ± 2.6	
c_1 = -1.69677865 ± 0.0000042	c_2 = 1.20943924 ± 0.000022
c_3 = - 0.50050321 ± 0.000191	c_4 = 0.29759884 ± 0.00132
c_5 = 0.01438024 ± 0.0023	c_6 = - 0.2733494 ± 0.043
c_7 = - 0.7999750 ± 0.133	c_8 = 3.140509 ± 0.22
c_9 = -11.96411 ± 2.4	c_{10} = 21.1058 ± 8.6
c_{11} = 87.2459 ± 18.1	c_{12} = - 711.9235 ± 24.2
s_0^C = - 0.0700 ± 0.0030	s_0^O = - 0.28727 ± 0.00085
t_0^C = [- 1.8427 ± 0.0030][a]	t_0^O = [- 1.7963 ± 0.0030]
t_1^C = [- 0.49446 ± 0.025]	t_1^O = [- 1.8457 ± 0.025]
t_2^C = [- 4.4008 ± 0.064]	t_2^O = [- 3.6433 ± 0.064]
t_3^C = [2.6873 ± 0.32]	t_3^O = [3.5365 ± 0.32]
t_4^C = [- 2.5569 ± 0.50]	t_4^O = [- 2.1059 ± 0.49]
u_1^C /10^6 m^{-1} = - 12.2564 ± 0.026	u_1^O / 10^6 m^{-1} = - 17.4410 ± 0.0192
u_2^C /10^6 m^{-1} = 118.384 ± 0.23	
u_3^C /10^6 m^{-1} = - 134.10 ± 5.0	

[a]Values of $t_j^{C,O}$ enclosed within brackets, fitted from data in table 2, are fixed in fits of frequency data.

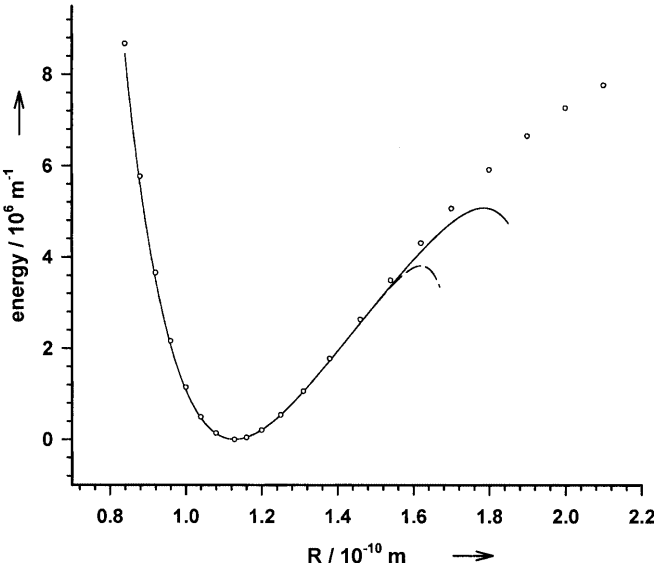

Fig. 2. V(z) as a *solid line* and V(x) as a *dashed line* for the potential energy of CO; the points marked with a *circle* represent the calculations reported in Table 2

These corrections take into account a condition that electrons follow imperfectly one or other atomic nucleus as the latter vibrate and rotate about the centre of mass. The eigenvalues [28, 29],

$$E_{vJ} = \sum_{k=0} \sum_{l=0} (Y_{kl} + Z_{kl}^{C} + Z_{kl}^{O})(v + 1/2)^k [J(J+1)]^l \ , \tag{10}$$

of that hamiltonian for each isotopic species contain as many term coefficients Y_{kl}, Z_{kl}^{C} and Z_{kl}^{O} of functionals of vibrational, v, and rotational, J, quantum numbers as are required to be consistent with coefficients c_j, s_j^C, s_j^O, t_j^C, t_j^O, u_j^C and u_j^O in radial functions up to a particular value of each individual subscript j, according to a fit with maximal statistical significance; further coefficients Y_{kl} and Z_{kl} are assumed to have negligibly small magnitudes and their values are taken as zero.

Data of rotational g factor, $g_r(R)$, and electric dipolar moment, $\vec{p}(R)$, in Table 2 are converted to values of $t^C(R)$ and $t^O(R)$ at each value of internuclear distance R according to these relations [30, 31]

$$t^{C}(R) = g_r(R)\mu/m_p - 2p(R)\mu/(eRM_O) \tag{11}$$

and

$$t^{O}(R) = g_r(R)\mu/m_p + 2p(R)\mu/(eRM_C) \ . \tag{12}$$

The resulting values of $t^C(R)$ and $t^O(R)$ are fitted to polynomials in z, for which degree four proved satisfactory in both cases. During fits of frequency data, values of coefficients $t_j^{C,O}$ in these polynomials are invariant; errors specified for $t_j^{C,O}$ in Table 4 represent their uncertainties from fitting to calculated data and play no part in analysis of frequency data. Fitted radial coefficients and other parameters appear in Table 4, in which, as elsewhere, each stated uncertainty implies an estimated single standard error; stated errors of k_e and R_e take into account errors in fundamental constants h and N_A; all calculations employ contemporary values of atomic masses and fundamental constants. We derive harmonic force coefficient k_e from $U_{1,0} = Y_{1,0}\mu^{1/2}$, and R_e likewise from $U_{0,1} = Y_{0,1}\mu$; $c_0 \equiv U_{1,0}^2/(4U_{0,1})$. The number of term coefficients Y_{kl} and $Z_{kl}^{C,O}$ required to fit frequencies and wave numbers of transitions sets a range of values of coefficients c_j, $s_j^{C,O}$ and $u_j^{C,O}$; further such coefficients are indeterminate on the basis of available data but are not assumed to be zero. Coefficients c_j,

Table 5 Experimental matrix elements of electric dipolar moment and Herman-Wallis coefficients for $^{12}C^{16}O$ in electronic ground state $X\ ^1\Sigma^+$

$v'-0$	$\langle v'\|\,p(x)\,\|0\rangle$ /10^{-30} C m	$C_0^{v'}$ / 10^{-2}	$D_0^{v'}$ / 10^{-4}	range
1 – 0	$-(3.5339\pm0.0053)\times10^{-1}$	0.024±0.021	—	P(27) – R(29)
2 – 0	$(2.2165\pm0.0027)\times10^{-2}$	0.533±0.014	0.44±0.10	P(28) – R(30)
3 – 0	$-(1.3633\pm0.0038)\times10^{-3}$	1.153±0.025	1.03±0.18	P(28) – R(31)
4 – 0	$(6.965\pm0.016)\times10^{-5}$	3.370±0.033	4.27±0.34	P(21) – R(23)

Table 6 Herman-Wallis coefficients calculated for $^{12}C^{16}O$ in electronic ground state $X\ ^1\Sigma^+$

v'	$C_0^{v'}$ /10^{-2}	$D_0^{v'}$/10^{-4}
0	0	-2.0553±0.0030
1	0.019543±0.000012	0.06740±0.00037
2	0.49736±0.00069	0.3483±0.0010
3	1.2143±0.0020	0.9865±0.0039
4	3.2688±0.0077	4.260±0.019

$1 \le j \le 8$, $U_{1,0}$ and $U_{0,1}$, all evaluated with satisfactory significance, were employed in subsequent analysis of spectral intensities. Excess digits are present in Table 4 to decrease rounding error in reproducing experimental values. With calculated points for energy, from Table 2 converted to units of reciprocal metres and offset relative to zero at the minimum, we plot in Fig. 2 the curve of function $V(z)$ truncated at c_{12}.

5 Analysis of intensity data

With knowledge of pressure, P, and temperature, T, of a sample at the time of its preparation, the area of each line was converted to a strength [2],

$$S_l = (1/Nl)\int \ln[I_0(\tilde{\nu})/I(\tilde{\nu})]\mathrm{d}\tilde{\nu}\ , \qquad (13)$$

in which $N = N_A P/RT$ is the total number of molecules of absorbing gaseous substance per unit volume in a sample, with length l of absorbing path through a sample, Avogadro's constant N_A and gas constant R; incident intensity at wave number $\tilde{\nu}$ is $I_0(\tilde{\nu})$ and transmitted intensity is $I(\tilde{\nu})$. Effects of nonideal gas and occupancy of vibrational states other than $X\ ^1\Sigma^+\ v=0$ are neglected, but the presence of isotopic variants is taken into account: natural abundance of $^{12}C^{16}O$ at 98.6646% is assumed and all parameters for spectral intensities stated here apply directly to this species. Components of both gaussian and lorentzian forms were generally allowed in the shape of a line being fitted, except for samples at the smallest pressures for which examination of shape indicated essentially a purely gaussian form. Measurements of parameters describing each individual spectral line – namely its wave number of maximum absorbance corresponding to its fitted profile, its stature, its full width at half its stature and its area – were entered into a spreadsheet according to branch P or R. Each area, implying the integral in Eq. (13), was converted into a line strength, according to Eq. (13), which was converted in turn into a square of a matrix element of electric dipolar moment according to [2]

$$S_l = \left(8\pi^3/3hc\right)[\exp(-hcE_{0J}/k_BT)/4\pi\varepsilon_0 Q] \times \tilde{\nu}_0[1-\exp(-hc\tilde{\nu}_0/k_BT)]|\imath||\langle v'J'|p(x)|0,J''\rangle|^2\ . \qquad (14)$$

In this equation apart from fundamental constants for speed of light in free space, c, the electrical permittivity of free space, ε_0, and Boltzmann's constant, k_B, E_{0J} is a rotational term of the lower state of a transition specified with quantum numbers $v''=0$ and J''; $\tilde{\nu}_0$ is the wave number of a transition from that state to another state characterised with quantum numbers $v'\ J'$; $\imath \equiv 1/2[J'(J'+1)-J''(J''+1)]$ is a running number of value $J''+1$ for a line in branch R or $-J''$ for a line in branch P. Rotational partition function Q, evaluated numerically as a direct sum over rotational states [2], includes contributions up to $J=50$; further contributions did not alter the value of Q for temperatures at which our experiments were conducted. In $|\langle v'J'|p(x)|0,J\rangle|^2$, which is the square of an experimental matrix element for a transition between states designated with quantum numbers $v'J'$ for upper state and 0, J'' for lower state, $p(x)$ is a radial function for electric dipolar moment of an absorber molecule in terms of reduced displacement $x=(R-R_e)/R_e$. Because the temperatures, pressures and lengths of absorbing path varied between experiments, we conducted all reductions of data directly on these matrix elements rather than on line strengths. For each band we fitted these matrix elements to a formula

$$|\langle v'J'|p(x)|0,J''\rangle|^2 = |\langle v'|p(x)|0\rangle|^2(1 + C_0^{v'}\imath + D_0^{v'}\imath^2) \ , \tag{15}$$

in which $|\langle v'|p(x)|0\rangle|^2$ is the square of the pure vibrational matrix element of electric dipolar moment; $C_0{}^{v'}$ and $D_0{}^{v'}$ are Herman–Wallis coefficients [2]. For all but the fundamental band we derived statistically significant values of coefficient $D_0{}^{v'}$. The resulting values of parameters appear in Table 5; each sign associated with a value of $\langle v'|p(x)|0\rangle$ therein is deduced from Herman–Wallis coefficients, as below.

With these magnitudes of pure vibrational matrix elements of electric dipolar moment, with $\langle 0|p(x)|0\rangle = (3.6632 \pm 0.0010)\times 10^{-31}$ C m derived from measurements on a molecular beam with electric resonance [32], of which its positive sign indicates relative electric polarity $^{-}CO^{+}$ at equilibrium internuclear distance R_e in accordance with the known rotational g factor and results of our calculations presented in Table 2, and with vibrational matrix elements of reduced displacement calculated analytically [33], we solve these five simultaneous linear equations,

$$\sum_{j=0}^{4} p_j \langle v'|x^j|0\rangle = \langle v'|p(x)|0\rangle, \quad 0 \le v' \le 4 \tag{16}$$

to yield coefficients p_j in an expansion for electric dipolar moment as follows:

$$\begin{aligned} p(x)/10^{-30}\,\mathrm{C\,m} &= \sum_{j=0}^{4} p_j x^j \\ &= (0.40792 \pm 0.00013) - (11.862 \pm 0.017)x \\ &\quad + (1.252 \pm 0.034)x^2 + (13.219 \pm 0.088)x^3 \\ &\quad - (3.06 \pm 0.27)x \end{aligned} \tag{17}$$

In Table 5, the signs of matrix elements $\langle v'|p(x)|0\rangle$ for $1 \le v' \le 4$, relative to a positive sign of $\langle 0|p(x)|0\rangle$, are chosen to achieve best agreement of values of coefficients $C_0{}^{v'}$, calculated with expressions [2] involving coefficients p_j and c_j and presented in Table 6, with empirical values listed in Table 5. We plot this function $p(x)$ in Fig. 3 with calculated points from Table 2 for comparison. Uncertainties in $C_0{}^{v'}$ and $D_0{}^{v'}$ specified in Table 6 are propagated from errors in coefficients p_j in Eq. (14), which are in turn propagated from errors in matrix elements $|\langle v'|p(x)|0\rangle|$ presented in Table 5; these uncertainties are estimated according to a Monte-Carlo method [34].

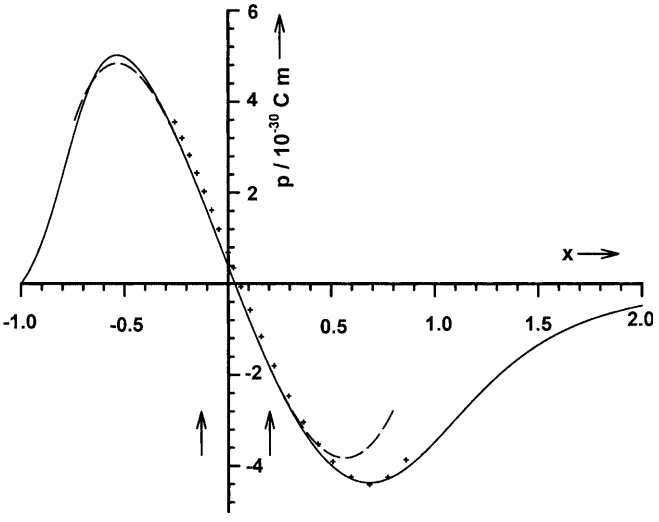

Fig. 3. $p(x)$ as a polynomial expansion according to Eq. (17) indicated with a *dashed line* and as a rational function according to Eq. (20) indicated with a *solid line*; points marked with a *cross* represent the calculations reported in Table 2

6 Discussion

In our experiments we recorded spectra of vibration–rotational bands of $^{12}C^{16}O$ in absorption from the vibrational ground state, $v'' = 0$, to the first four vibrationally excited states, with $1 \le v' \le 4$. All these bands had been previously recorded, yielding not only wave numbers of individual lines but also their strengths, as well as strengths of some bands from broadened or unresolved lines. We sought to observe also the fourth overtone band, 5–0, but discerned no signal at expected wave numbers; a previous search [35] with product of length of absorbing path and pressure equal to 3,000 m bar was equally unsuccessful; 1 bar = 10^5 N m^{-2}. With a corresponding product of only 26 m bar we managed to detect band 4–0 with sufficient absorbance of lines to measure their areas, in contrast to a product of at least 500 m bar employed with photographic detection [35]. Our wave numbers for the latter band (Table 3) are about 30 times as precise as those reported by Herzberg and Rao [35], but they otherwise agree satisfactorily. For band 4–0, our maximum length of path through absorbing sample, 107 m, required that we employ pressures up to 1.08×10^5 N m^{-2}; under these conditions a shift of each spectral line to smaller wave number is discernible with increasing total pressure of pure sample. The mean shift is (-0.648 ± 0.073) m^{-1} bar^{-1}; all wave numbers in Table 3 result from application of that correction to mean wave numbers from spectra obtained for samples at pressures in a range/10^5 N m^{-2} [0.27, 1.08].

Because, for bands other than that for 4–0 that we measured, our wave numbers are no more precise than those previously collected from the literature [15], we omitted our data from a global fit of single transitions in spectra measured in both absorption and emission. Our fit of 16,947 measurements of frequencies and wave numbers of pure rotational and vibration–rotational transitions of CO in isotopic species $^{12}C^{16}O$, $^{12}C^{17}O$, $^{12}C^{18}O$, $^{13}C^{16}O$, $^{13}C^{17}O$, $^{13}C^{18}O$ and $^{14}C^{16}O$ up to maximum $v' = 41$ and maximum $J' = 133$ required, with ten constrained parameters, only 18 adjusted parameters to reproduce those data within, on average, their precision of measurement: the reduced standard deviation of the best fit is 0.95. This extent of data reduction is consequently almost as great as for GeO, for which 5,484 distinct pure rotational or vibration–rotational transitions of ten isotopic species up to $v' = 8$ and $J' = 104$ required, with two constrained parameters, only

six fitted parameters [36] to reproduce satisfactorily all data.

Although function $V(z)$ with coefficients c_j with $0 \le j \le 12$ specified in Table 4 proves satisfactory for a purpose of reproducing frequencies of transitions involving vibration–rotational states having spectral terms up to 8×10^6 m^{-1}, corresponding roughly to $v=41$, a curve of that function truncated at c_{12} appears to deviate appreciably from large calculated energies according to Table 2 and reaches a maximum about 5×10^6 m^{-1}, as shown in Fig. 2. A curve of function $V(x)$, in terms of an alternative reduced displacement coordinate x for which coefficients a_j, $j \le 12$, are merely converted accurately from fitted coefficients c_j, appears to deviate even worse from calculated points and reaches a maximum about 3.7×10^6 m^{-1}, despite a notable adequacy of these functions $V(x)$ and $V(z)$ to reproduce spectral data involving transitions to states with spectral terms up to 8×10^6 m^{-1}. These appearances are deceptive, being artefacts of truncated polynomials; they arise because plotting such functions $V(z)$ or $V(x)$ requires further coefficients to be set to zero, whereas no such constraint is applicable to use of c_j or a_j in fitting data according to present practice. A claim [37] to reproduce spectral transitions up to $v'=41$ with coefficients a_j up to only $j=10$ is remarkable because a_{10} occurs in a purely vibrational term coefficient $Y_{k,0}$ first for $k=6$, or $Y_{6,0}$, whereas with separate empirical parameters U_{kl} purely vibrational coefficients $U_{k,0}$ up to $k=9$, implying $U_{9,0}=Y_{9,0}\mu^{9/2}$ and a_{16} or c_{16}, are required [38]. In this regard, our own achievement in requiring coefficients up to only c_{12} might be almost as remarkable. An explanation might be that those parameters [38] appear highly artificial, possibly because constraints were applied in an inconsistent manner: values of those parameters U_{kl} differ significantly from corresponding values derived from coefficients c_j in an entirely consistent manner in the present work.

Radial coefficients $u_j^{C,O}$ in Table 4 pertain formally to adiabatic effects, whereas coefficients $s_0^{C,O}$ pertain to nonadiabatic vibrational effects; as coefficients $t_j^{C,O}$ are obtained from calculated values of rotational g factor and electric dipolar moment, there is no question about their relation to nonadiabatic rotational effects. As we employ analytic expressions for $Z_{kl}^{C,O}$ derived from a comprehensive hamiltonian [28] in which all these adiabatic and nonadiabatic effects of order m_e/M – which is a ratio of electronic and nuclear masses – with respect to other terms are included explicitly, our values of coefficients of $s_0^{C,O}$ and $u_j^{C,O}$ can possess greater physical significance than preceding values of coefficients [15, 37, 39] deduced with a hamiltonian involving parameters of only two types: in the latter case, coefficients of radial functions that have as factor $J(J+1)$ contain, in unknown proportions, contributions from both nonadiabatic rotational and nonadiabatic vibrational effects, whereas another auxiliary radial function contains contributions from both nonadiabatic and adiabatic vibrational effects [28]. Comparison of parameters for extra-mechanical effects evaluated by Coxon and Hajigeorgiou [39], which comprise nine parameters of type $u_j^{C,O}$ but only two of type $t_j^{C,O}$, with four $u_j^{C,O}$ and ten $t_j^{C,O}$ in Table 4 indicates clearly that their numerical approach fails to distinguish properly between vibration–rotational and further rotational contributions to extra-mechanical effects [2, 40]; in particular, in excluding $t_0^{C,O}$ they ignore the important contribution of the rotational g factor [16], for which a value is well established for CO [41]. Reservations previously expressed [37] about the quality of this data reduction [39] remain to be assuaged.

In any case one must bear in mind that a radial function, whether for potential energy or dipolar moment or another molecular property, is not a physically observable quantity, but merely an artefact of an approximate ansatz for calculation involving separate treatment of electronic and nuclear motions within a molecule. According to such a context, our function for potential energy defined in Table 4 fulfils its purpose if reproduction of measured frequencies of transitions is successful, regardless whether an artefactual curve appears to have an expected form. Although purely calculated electronic energies, as in Table 2, might be applied to calculate spectral terms, the corresponding wave numbers of transitions differ from experimental measurements typically by thousands of times the errors of measurement. In contrast to purely numerical fits of spectral data involving innumerable solutions of Schrödinger's temporally independent equation – one solution for each vibration–rotational state of each isotopic species, our analytic approach enables direct evaluation of spectral terms – and their differences that constitute frequencies or wave numbers of transitions – merely on substitution of fitted values of radial coefficients, as in Table 4, into well defined algebraic expressions Y_{kl} and Z_{kl} [2, 40], which are equivalent to those of Dunham [42] but much more extensive, and which are readily available in computer code [43] or which can be generated rapidly and accurately with reliable procedures for symbolic computation [33]. Parameters c_j in Table 4 imply 47 finite values of U_{kl} and other radial coefficients there imply at least 18 values of $\Delta_{kl}^{C,O}$ which are combinations of Z_{kl}, voluminous subsidiary data that we refrain from presenting here. In contrast, George et al. [38] tabulated only 31 values of U_{kl} and 12 values of $\Delta_{kl}^{C,O}$, some of which have magnitudes smaller than those of parameters that they omitted. With expressions for Y_{kl} and Z_{kl} readily available [43] or generated [33], for purposes of reproducing frequencies of transitions one can simply substitute values of radial coefficients from Table 4 into those expressions in Eq. (10) to obtain any required differences of spectral terms $E_{v,J}$. Experience during progressive assignments of new spectra of other compounds demonstrates that these radial coefficients possess typically a predictive capacity for energies of states moderately beyond those involved in fitting those parameters. At the very least, values in Table 4 of coefficients c_j, $1 \le j \le 8$, which are valid for $R/10^{-10}$ m in a range [0.9, 1.5], suffice for purposes of construction of a radial function for electric dipolar moment. Because coefficients $s_j^{C,O}$ and $u_j^{C,O}$ reflect essentially only precise data for isotopic variants with ^{13}C and ^{17,18}O involving vibrational states with $v \lesssim 3$, their maximum range of validity is $1.05 \le R/10^{-10}$ m ≤ 1.25; coefficients $t_j^{C,O}$ are valid according to their stated uncertainties within a range indicated in Table 2.

For the purpose of determining the centre of a narrow and symmetric spectral line, or the wave number at which absorption is maximum, the shape of that line is somewhat immaterial, as long as the ratio of signal to noise is sufficiently large to prevent significant distortion. For each spectrum for which we fitted the lines to evaluate wave number and area, the latter to be converted subsequently into a line strength, we tested whether the line shape is best represented as a pure lorentzian form – characteristic of lines broadened because of molecular collisions – or as a pure gaussian form – characteristic of Doppler effects in absence of collisional broadening – or by a sum of lorentzian and gaussian contributions; we found generally that the latter combination provides the most reliable fit, although a lorentzian contribution is dominant under most conditions. We find thereby that our line strengths agree satisfactorily with those in the literature measured at directly comparable temperature; for instance, for band 3–0, a ratio of our line strengths in one experiment to those reported by Picque et al. [44] at nearly the same temperature is 0.997 ± 0.027, with negligible systematic discrepancy. As temperatures/K of samples in our experiments have a range [296.25, 303.5], even though the temperature was constant to within 0.6 K within a particular experiment for which data were accepted, we converted all line strengths to vibration–rotational matrix elements of electric dipolar moment according to Eq. (14) and performed analysis of intensities on that basis. Revealed from data of separate experiments, there is inevitable scatter in individual values of these matrix elements, varying from about 1% for the most intense lines in a band to about 20% for the weakest measurable lines; fitting these matrix elements for 45–60 lines with at most three parameters according to Eq. (15) nevertheless yields highly significant parameters (Table 5).

For band 1–0 our value of $|\langle 1|p(x)|0\rangle|$ corresponds to a band strength $(1.028 \pm 0.002)\times10^{-19}$ m, which agrees satisfactorily with a generally accepted value $(1.022 \pm 0.036)\times10^{-19}$ m derived by Varanasi and Sarangi [45] and with other data [3, 4, 5]. Herman–Wallis coefficient $C_0{}^1$ has such a small value that it can be measured only with difficulty; our value $(2.4 \pm 2.1)\times10^{-4}$ appears poorly significant, in that the standard error of the value is comparable with the value, but only because that magnitude is so small. From measurements using a technique similar to that in our experiments, Bailly et al. [46] estimated a value $C_0{}^1 = (1.74 \pm 0.04)\times10^{-4}$. Both these experimental values agree roughly with a calculated value 1.95×10^{-4} in Table 6. Attempts to evaluate significantly coefficient $D_0{}^1$ were unsuccessful as a result of its small magnitude.

For band 2–0 our value $|\langle 2|p(x)|0\rangle| = (2.2165 \pm 0.0027)\times10^{-32}$ C m in Table 5 essentially coincides with a value $(2.2115 \pm 0.0067)\times10^{-32}$ C m [47] derived from a generally accepted strength of this band; the associated value of Herman–Wallis coefficient $C_0{}^2 = (0.545 \pm 0.007)\times10^{-2}$ [47] agrees likewise with our measured value of $(0.533 \pm 0.014)\times10^{-2}$ in Table 5 and reasonably well with a calculated value in Table 6. As we exerted particular care with measurement of this band, both in preparation of sample to ensure utmost accuracy of measurement of pressure and in analysis of intensity data that span a greater range of lines in both branches than in previous reports, we are confident that our result is valid.

For band 3–0 we compare our values, in Table 5, of $|\langle 3|p(x)|0\rangle|$ and Herman–Wallis coefficients directly with those reported from contemporary experiments: $|\langle 3|p(x)|0\rangle| = (1.3676 \pm 0.0067)\times10^{-33}$ C m and $C_0{}^3 = (1.323 \pm 0.046)\times10^{-2}$ from lines in only branch R up to $J'' = 20$ [8]; $|\langle 3|p(x)|0\rangle| = (1.3642 \pm 0.0006) \times10^{-33}$ C m, $C_0{}^3 = (1.204 \pm 0.015)\times10^{-2}$ and $D_0{}^3 = (1.08 \pm 0.15)\times10^{-4}$ from lines in branches P and R, up to $J'' = 20$ in both cases [9], whereas our parameters are based on measurements of more lines in each branch. Agreement among these three values of $|\langle 3|p(x)|0\rangle|$ and $C_0{}^3$ and two values of $D_0{}^3$ and of experimental and calculated values of coefficients $C_0{}^3$ and $D_0{}^3$ is satisfactory.

For band 4–0 we compare our values, in Table 5, directly with those reported from old measurements [48]: $|\langle 4|p(x)|0\rangle| = (6.712 \pm 0.027)\times10^{-35}$ C m; $C_0{}^4 = (3.55 \pm 0.08)\times10^{-2}$ and $D_0{}^3 = (4.81 \pm 0.48)\times10^{-4}$ from lines in branches P, up to $J'' = 16$, and R, up to $J'' = 14$. Our magnitude of $|\langle 4|p(x)|0\rangle|$ is slightly greater than the earlier value [48]; agreement is otherwise satisfactory between experimental values of coefficients $C_0{}^4$ and $D_0{}^4$ and with corresponding calculated values in Table 6.

Agreement of our results for these bands of CO in this work, just as of O_2 in preceding work [7], with accepted results in the literature [3, 4, 5] indicates that our new measurements are reliable. We thus combined these four matrix elements of electric dipolar moment, one from each band for a transition from vibrational ground state $v'' = 0$ to a vibrationally excited state with $1 \le v' \le 4$, with a value for the matrix element $\langle 0,1|p(x)|0,1\rangle/10^{-31}$ C m $= 3.6625 \pm 0.0010$ derived from experiments [32] on a molecular beam with electric resonance, essentially analogous to use of the Stark effect on a pure rotational transition but more precise; a measurement [49] of the intensity of a pure rotational transition $J' = 1 \Leftarrow J'' = 0$ in the ground vibrational state yielded the same result but with inferior precision. For use in our calculations, we adjusted that matrix element evaluated from experiment [32] to take into account a vibrational contribution of order $(U_{0,1}/U_{1,0})^2$. On a basis of those five matrix elements derived from, or consistent with, analysis of intensities of pure rotational or vibration–rotational transitions, we evaluated a function for electric dipolar moment in Eq. (17) for $^{12}C^{16}O$ by solving five linear relations implied in Eq. (16). We inferred the signs of $\langle v'|p(x)|0\rangle$ from the best agreement of Herman–Wallis coefficients $C_0{}^{v'}$ and $D_0{}^{v'}$ calculated using $\langle v'|p(x)|0\rangle$ and coefficients p_j in Eq. (13); as illustrated for the case of HCl [2], this method is sensitive to those signs. Agreement between calculated, in Table 6, and experimental, in Table 5, values of $C_0{}^{v'}$ and $D_0{}^{v'}$ is satisfactory, indicating both the quality of our measurements of intensity and an adequate theoretical treatment. We verified that values of matrix elements $|\langle v'|p(x)|0\rangle|$ according to Table 5

combined with values of ${C_0}^{v'}$ and ${D_0}^{v'}$ from Table 6 reproduce our measured areas of spectral lines generally within the uncertainties of measurement. Equation (16) is equally applicable to calculation of intensities of not only pure rotational transitions of $^{12}C^{16}O$ in vibrational states up to $v=4$, but also, to the extent that adiabatic and nonadiabatic effects are small relative to error of measurement, spectral transitions of CO in its isotopic variants with apt values of vibrational matrix elements.

Figure 3 shows a slight, but distinct, systematic offset between calculated values of electric dipolar moment from Table 2 and the function for $p(x)$ according to Eq. (17). To eliminate possible inconsistency between experimental and calculated quantities during a final fit of experimental wave numbers and frequencies, we subtracted 0.27693×10^{-30} C m – the difference between experimental and calculated values of $p(x)$ at $x=0$ or $R=R_e$ – from calculated values in generating final values of ${t_j}^C$ and ${t_j}^O$ presented in Table 4; we likewise subtracted 0.01435 from calculated values of rotational g factor from Table 2 in constructing those values of ${t_j}^C(R)$ and ${t_j}^O(R)$ to ensure conformity with an experimental value $g_r=\langle 0,1|g_r(x)|0,1\rangle=-0.26895$ [41], after correction for vibrational averaging.

Coefficients ${u_j}^{C,O}$ in Table 4 pertain formally to adiabatic effects, whereas coefficients ${s_0}^{C,O}$ pertain to nonadiabatic vibrational effects. According to Eq. (18) [29],

$$p_1 = {}^1\!/_2 e R_e ({s_0}^O - {s_0}^C) \ , \tag{18}$$

into which we insert a value of R_e from Table 4 and a value of coefficient p_1 from Eq. (17), the difference ${s_0}^O - {s_0}^C$ is 1.31, whereas that difference according to Table 4 is –0.217. Although coefficients ${u_1}^{C,O}$ are nominally free from influence of nonadiabatic vibrational effects [40], and although nonadiabatic rotational effects are taken quantitatively into account through quantum-chemical calculations of $g_r(R)$ and $p(R)$, effects of s_0 and u_2 enter expressions for Z_{kl} at the same level. These effects are evidently not effectively discriminated in our present reduction of frequency data, likely because of the paucity of wave numbers of transitions of CO containing ^{17}O or ^{18}O beyond the ground vibrational state; association of values of ${s_0}^{C,O}$, ${u_2}^C$ and ${u_3}^C$ with particular terms in the hamiltonian (Eq. 4) is hence uncertain.

In an analysis lacking recently published data on band intensities, Kiriyama and Rao [10] claim to have derived a function for the electric dipolar moment of $^{12}C^{16}O$ by fitting, in total, 183 matrix elements of individual lines. In the case of band 1–0, they tabulate 57 such matrix elements, each with five significant digits, which they claim that Varanasi and Sarangi measured [45], although the latter authors present explicitly only 19 line strengths, each reported with at most three significant digits. For band 4–0, they [10] likewise tabulate 40 matrix elements, attributed to measurements of Chackerian and Valero [48], but the latter authors list only 32 line strengths; uncertainties in the latter matrix elements are stated to vary in a range by over a factor of 115, but Kiriyama and Rao provide no indication that such variation is taken into account in their work [10]. For comparison with our function in Eq. (17), their function for electric dipolar moment is

$$\begin{aligned} p(x)/10^{-30}\text{C m} = {} & (0.409817\pm0.000013) \\ & -(12.0576\pm0.0044)x \\ & +(0.10620\pm0.00076)x^2 \\ & +(9.7367\pm0.0029)x^2 \\ & -(14.0565\pm0.0059)x^4. \end{aligned} \tag{19}$$

Despite an evident disparity in values of coefficients p_2, p_3 and p_4 between Eqs. (17) and (19), a curve of the latter function practically coincides with the curve of Eq. (17) within a maximum range of definition, $1.0 \le R/10^{-10}\ \text{m} \le 1.3$ or $-0.11 \le x \le 0.15$, indicated with vertical arrows in Fig. 3, that corresponds to the interval between classical turning points for vibrational state with $v=4$. This curve of Eq. (19) lacks a maximum at about $R=1.8\times10^{-10}$ m or $x=0.7$ displayed by both calculated points in Table 2 and, perhaps fortuitously, the dashed curve of Eq. (17), as shown in Fig. 3. To bestow the proper behaviour on a function for electric dipolar moment, such that it is zero at $R=0$ and its approach to that limit is proportional to R^3, and such that its approach to a zero limit as $R\to\infty$ is proportional to R^{-4}, we convert Eq. (17) to a rational function [50]:

$$p(x)/10^{-30}\text{C m} = \frac{0.40792(1-27.93551x-28.93551x^2)}{1+1.1444x+1.2748x^2+1.1517x^3+C_\infty x^6}. \tag{20}$$

With $C_\infty=2.0$, this curve, marked as a solid line in Fig. 3, passes near calculated points from Table 2 that define a maximum near $x=0.7$. Although this function is only qualitatively meaningful beyond its stated range of definition, it might serve to predict intensities for transitions in absorption from the vibrational ground state to excited states beyond $v=4$. In comparison, an alternative rational function [51] has much larger extrema at $x=\pm0.75$, thus not passing near calculated points about $x=0.7$, and fails to tend to a zero limit at $x=-1$ or $R=0$. Equation (20) hence provides likely the best basis at present to predict intensities of vibration–rotational transitions in absorption or emission for a moderately large range of v and J.

In past analyses of these intensity data [6] we employed serial processing of measurements with programs in Basic and Fortran, after forming analytic expressions of matrix elements [52] and Herman–Wallis coefficients with a symbolic processor and their conversion into Basic or Fortran code. In the present work, use of a commercial spreadsheet to record data about each spectral line – its wave number, stature, width and area (derived with Grams software) – followed by collective processing to form line strength and matrix element, proved an efficient mechanism to handle numerous data, typically 8–15 acceptable spectral records of samples under various conditions for each of four main bands each comprising 45–60 lines. In subsequent processing,

we copied columns of wave numbers of vibration–rotational transitions, or matrix elements squared, $|\langle v'J'|p(x)|0,\ J''\rangle|^2$, from that spreadsheet to become vectors with Maple software for symbolic computation, with which we made directly all further calculations. Algebraic expressions [33] of vibrational matrix elements $\langle v'|x^j|0\rangle$ and of Herman–Wallis coefficients ${C_0}^{v'}$ and ${D_0}^{v'}$ were generated directly within Maple, into which we substituted numerical values of parameters from Table 4, calculated separately with the Fortran program Radiatom [40] with precision 32 decimal digits, and from Table 5 as fitted with Maple, and we calculated thereby the corresponding uncertainties in an error analysis [34]. As numerical precision in Maple can be set arbitrarily great, there is no loss of precision in calculations with decimal numbers; we used 16–24 decimal digits as apt for various calculations. Such calculation within Maple also precludes problems of conversion or transfer of expressions from one language to another. Although fitting of spectral frequencies and wave numbers to derive parameters as in Table 4 can also be effected within Maple, the duration of processing about 17,000 data for CO is inconveniently protracted.

7 Conclusion

Assisted with values of rotational g factor from quantum-chemical calculation as a function of internuclear distance, we fitted frequency and intensity data to reproduce essential features of vibration–rotational spectra of CO in absorption in a range/$10^5\,m^{-1}$ [1.5, 9.0]; calculations of energy and electric dipolar moment serve for comparison with experimentally derived quantities. Of parameters pertaining to potential energy from frequency data and electric dipolar moment from intensity data, only 18 fitted values with a further ten constrained coefficients in seven radial functions suffice to reproduce 16,947 measurements of frequency and wave number comparable with their uncertainties, and four fitted parameters with a further adopted value in a formula for electric dipolar moment as a function of internuclear distance suffice to reproduce about 220 absolute intensities of lines in vibration–rotational bands.

Acknowledgements. We are grateful to G. Winnewisser for providing frequencies of transitions of $^{12}C^{17}O$ and $^{13}C^{17}O$ before publication. Y.P.L. thanks the National Science Council of Republic of China for support of this work at National Tsing Hua University in project NSC90-2113-M-007-008. S.P.A.S. thanks the Danish Natural Science Research Council for support of this work at University of Copenhagen through grants 9901973, 9701136 and 0001920.

References

1. Winnewisser G, Herbst E, Ungerechts H (1992) In: Rao KN, Weber A (eds) Spectroscopy of the Earth's atmosphere and interstellar medium. Academic, Boston, p 423
2. Ogilvie JF (1998) The vibrational and rotational spectrometry of diatomic molecules. Academic, London
3. Pugh LA, Rao KN (1976) In: Rao KN (ed) Molecular spectroscopy: modern research. Academic, New York, pp 165–181
4. Smith MAH, Rinsland CP, Fridovich B, Rao KN (1985) In: Rao KN (ed) Molecular spectroscopy: modern research. Academic, New York, p 111
5. Smith MAH, Rinsland CP, Devi VM, Rothman LS, Rao KN (1992) In: Rao KN, Weber A (eds) Spectroscopy of the Earth's atmosphere and interstellar medium. Academic, Boston, p 253
6. Ogilvie JF, Lee YP (1989) Chem Phys Lett 159: 239
7. Cheah SW, Lee YP, Ogilvie JF (2000) J Quant Spectrosc Radiat Transfer 64: 467
8. Henningsen J, Simonsen H, Mogelberg T, Trudso E (1999) J Mol Spectrosc 193: 354
9. Picque N, Guelachvili G, Dana V, Mandin JY (2000) J Mol Struct 517: 427
10. Kiriyama F, Rao BS (2000) J Quant Spectrosc Radiat Transfer 65: 673
11. Winnewisser G, Belov SP, Klaus T, Schieder R (1997) J Mol Spectrosc 184: 468
12. Klapper G, Lewen F, Gendriesch R, Belov SP, Winnewisser G (2000) J Mol Spectrosc 201: 124
13. Klapper G, Lewen F, Belov SP, Winnewisser G (2000) Z Naturforsch 55a: 441
14. Klapper G, Lewen F, Gendriesch R, Belov SP, Winnewisser G (2001) Z Naturforsch 56a: 329
15. Ogilvie JF, Ho MCC (1993) Chin J Phys 31: 721
16. Ogilvie JF, Oddershede J, Sauer SPA (2000) Adv Chem Phys 111: 475
17. Guelachvili G for IUPAC commission on molecular structure and spectroscopy (1996) Pure Appl Chem 68: 193
18. Olsen J, Jørgensen P (1985) J Chem Phys 82: 3235
19. Sauer SPA, Packer MJ (2000) In: Bunker PR, Jensen P (eds) Computational molecular spectroscopy. Wiley, London, p 221
20. van Duijneveldt FB (1971) IBM Tech Rep RJ 945
21. Dunning TH (1989) J Chem Phys 90: 1007
22. Roos BO (1987) Adv Chem Phys 69: 399
23. Helgaker T, Jensen HJA, Joergensen P, Olsen J, Ruud K, Aagren H, Bak KL, Bakken V, Christiansen O, Dahle P, Dalskov EK, Enevoldsen T, Fernandez B, Heiberg H, Hettema H, Jonsson D, Kirpekar S, Kobayashi R, Koch H, Mikkelsen KV, Norman P, Packer MJ, Ruden TA, Saue T, Sauer SPA, Sylvester–Hvid KO, Taylor PR, Vahtras O (1999) Dalton release 1.1 (2000), an electronic structure program. http://www.kjemi.uio.no/ software/dalton/dalton.html
24. Mink J, Ayoub A, Kemeny G, Kremo R, Kling F (1980) Spectrochim Acta Part A 36: 151
25. Mink J, Ayoub A, Kemeny G, Kling F (1981) J Mol Spectrosc 86: 258
26. George T, Saupe S, Wappelhorst MH, Urban W (1994) Appl Phys B 59: 159
27. Picque N, Guelachvili G (1997) J Mol Spectrosc 185: 244
28. (a) Fernandez FM, Ogilvie JF (1992) Chin J Phys 30: 177; (b) Fernandez FM, Ogilvie JF (1992) Chin J Phys 30: 599
29. Herman RM, Ogilvie JF (1998) Adv Chem Phys 103: 287
30. Ogilvie JF, Liao SC (1994) Chem Phys Lett 226: 281
31. Sauer SPA (1998) Chem Phys Lett 297: 475
32. Muenter JS (1975) J Mol Spectrosc 55: 490
33. Fernandez FM, Ogilvie JF (1998) MapleTech 5: 42 http://www.mapleapps.com/categories/science/physics/html/dimolspc.html
34. Ogilvie JF (1984) Comput Chem 8: 205
35. Herzberg G, Rao KN (1949) J Chem Phys 17: 1099
36. Ogilvie JF, Uehara H, Horiai K (1999) Can J Anal Sci Spectrosc 44: 141
37. Diaz CG, Tipping RH (1994) J Mol Spectrosc 163: 58
38. George T, Urban W, LeFloch A (1994) J Mol Spectrosc 165: 500
39. Coxon JA, Hajigeorgiou PG (1992) Can J Phys 70: 40
40. Ogilvie JF (1994) J Phys At Mol Opt Phys B 27: 47
41. Meerts WL, de Leeuw FH, Dymanus A (1977) Chem Phys 22: 319

42. Dunham JL (1932) Phys Rev 41: 721
43. Ogilvie JF (1983) Comput Phys Commun 30: 101
44. Picque N, Guelachvili G, Dana V, Mandin JY (2000) J Mol Struct 517: 427
45. Varanasi P, Sarangi S (1975) J Quant Spectrosc Radiat Transfer 15: 473
46. Bailly D, Rossetti C, Thibault F, LeDoucen R (1991) J Mol Spectrosc 148: 329
47. Chandraiah G, Hebert GR (1981) Can J Phys 59: 1367
48. Chackerian C, Valero FPJ (1976) J Mol Spectrosc 62: 338
49. Fabian M, Morino I, Yamada KMT (1997) J Mol Spectrosc 185: 422
50. Kirschner SM, LeRoy RJ, Ogilvie JF, Tipping RH (1977) J Mol Spectrosc 65: 306
51. Goorvitch D, Chackerian C (1994) Astrophys J Supp Ser 91: 483
52. Bouanich JP, Ogilvie JF, Tipping RH (1986) Comput Phys Commun 39: 439